

Automatic Horizontal Fusion for GPU Kernels

Ao Li
University of Toronto
leo@cs.toronto.edu

Bojian Zheng
University of Toronto
bojian@cs.toronto.edu

Gennady Pekhimenko
University of Toronto
pekhimenko@cs.toronto.edu

Fan Long
University of Toronto
fanl@cs.toronto.edu

Abstract—We present automatic horizontal fusion, a novel optimization technique that complements the standard kernel fusion techniques for GPU programs. Unlike the standard fusion, whose goal is to eliminate intermediate data round trips, our horizontal fusion technique aims to increase the thread-level parallelism to hide instruction latencies. We also present HFUSE, a new source to source CUDA compiler that implements automatic horizontal fusion. Our experimental results show that the horizontal fusion can speed up the running time by 2.5%-60.8%. Our results reveal that the horizontal fusion is especially beneficial for fusing kernels with instructions that require different kinds of GPU resources (e.g., a memory-intensive kernel and a compute-intensive kernel).

I. INTRODUCTION

Graphics Processing Units (GPUs) are widely used to speed up deep learning tasks, scientific computation, and even cryptocurrency mining. Each GPU comes with dozens to hundreds of processing cores enabling thousands of threads running in parallel to achieve much higher computational throughput than a normal CPU [1]. Despite of the rapid advancement of the GPU hardware, the applications running on GPUs are always hunger for more performance. For example, training state-of-the-art deep learning models like ResNet-50 can take 2 hours on 8 Tesla V100 GPUs [2].

To speed up computational tasks running on GPUs, especially for deep learning, people have developed many optimization techniques at the software level [3–8]. Among these techniques, *Kernel fusion* is a popular and effective one [9–14] and it is adopted by almost all deep learning frameworks [4–8, 15, 16]. In GPU programs, a large computational task (e.g., training a neural network) is broken down into multiple *kernels*, each of which corresponds to a small parallelizable sub-task that will be dispatched to GPUs to execute. The idea of kernel fusion is to combine two or more kernels into one large but equivalent kernel to potentially improve the overall performance.

The standard kernel fusion technique in the deep learning frameworks combines kernels *vertically*. The fused kernel will have the same number of threads as the two original kernels. Each thread of the fused kernel sequentially combines the instructions of the corresponding threads of the original kernels [4–7, 16]. The potential performance advantage is from reducing expensive data round trips to the GPU device memory — without the fusion the first original kernel needs to write its output to the memory for the second kernel to read.¹

¹For tiny kernels, both vertical and horizontal kernel fusion also reduces kernel launch overhead.

Therefore the standard kernel fusion application is typically limited to neighboring kernels in the data dependency graph, i.e., the output of one kernel is the input of another kernel.

A. HFUSE: *Horizontal Fusion*

We present a novel optimization technique, *automatic horizontal fusion*. Unlike the standard fusion that aims to eliminate intermediate data round trip, our horizontal kernel fusion enables the fused kernel to better utilize GPU resources and to better hide instruction latencies. The horizontal fusion complements the standard vertical fusion in its application scenarios — horizontally fusing two kernels is beneficial if the two kernels contain instructions that require different types of GPU resources (e.g., a memory-intensive kernel and a compute-intensive kernel).

We also present HFUSE, a source to source CUDA compiler that implements our automatic horizontal fusion technique. Given the CUDA source code of two kernels, HFUSE automatically produces the horizontally fused kernel that is functionally equivalent to the two but runs potentially faster. In the horizontally fused kernel, the threads are partitioned into two intervals based on their thread ids. Each interval corresponds to threads for the computation of one original kernel. The fused kernel combines the instructions of the original kernels with branch statements. The branch conditions checks the current thread id to dispatch the execution to the path of the corresponding kernel. Because threads of two original kernels coexist in parallel during the execution, the horizontal fusion exploits the thread-level parallelism. It enables the thread scheduling hardware (e.g., warp schedulers in NVIDIA GPUs) to automatically interleave instructions from different kernels to hide instruction latencies.

One challenge of implementing the automatic horizontal fusion is to handle synchronization barriers. A typical CUDA barrier stalls the execution of all threads in a thread block of a kernel until all of the threads reach the barrier. Because a fused kernel contains threads derived from both of the original kernels, such barriers from one of the original kernels will impact the thread execution of another. Another challenge HFUSE faces is to identify the best way to partition the thread space of a fused kernel, which is shared by the instructions of the two original kernels. Because the partition scheme determines how the execution of the original kernels co-exists in GPU, it may significantly impact the performance of the fused kernel.

To address the first challenge, HFUSE combines inline PTX assembly instructions with instrumented branch conditions to implement special barriers for the thread sets that correspond to original kernels. To address the second challenge, HFUSE operates with an automatic profiling technique. Given the expected input sizes of two original kernels, HFUSE will automatically search the best thread space partition.

B. Experimental Results

We evaluate HFUSE with 5 deep learning computational kernels extracted from PyTorch [16] and 4 cryptography computational kernels collected from open source cryptocurrency mining programs [17, 18]. In total, we apply HFUSE to fuse 16 pairs of kernels. We compare the running time of the HFUSE fused kernel with the native kernels and the kernels fused in the standard vertical way. Our experimental results show that the HFUSE fused kernels run up to 60.8% faster than the native kernels; for 7 out of the 16 pairs on 1080Ti GPU and 6 out of the 16 pairs on V100 GPU, the HFUSE fused kernels outperform both the vertically fused kernels and the native kernels. Our results reveal that the speed up of the fused kernel comes from interleaving different kernel computations to hide instruction latencies.

Our results also reveal the trade-off between the thread-level and the block-level parallelism for kernel fusion. On one hand, the horizontal fusion enables the thread scheduler to interleave instructions with the improved thread-level parallelism. On the other hand, The fused kernel will require more register and shared memory resources than individual kernels. If such additional requirement exceeds a certain breakpoint, it may cause less thread blocks being scheduled to each core to reduce the block-level parallelism. One could view HFUSE as a technique to navigate this trade-off. See Section IV-C.

C. Contribution

This paper makes the following contributions:

- **Automatic Horizontal Fusion:** This paper presents automatic horizontal fusion, a novel optimization technique that is orthogonal to the standard vertical kernel fusion. The horizontal fusion can enable the GPU hardware to effectively interleave instructions from two original kernels to hide instruction latencies.
- **HFUSE:** This paper presents the design and implementation of HFUSE, a novel source to source CUDA compiler that implements automatic horizontal fusion.
- **Optimization Scenarios:** This paper identifies the scenarios for applying the horizontal fusion technique. Our results show that horizontal fusion is mostly beneficial when fusing two kernels with instructions that have long latencies and that require different types of GPU resources.

The remaining of this paper is organized as follows. Section II presents an overview of the horizontal kernel fusion technique and a motivating example of applying HFUSE to fuse two kernels. Section III presents the design of HFUSE.

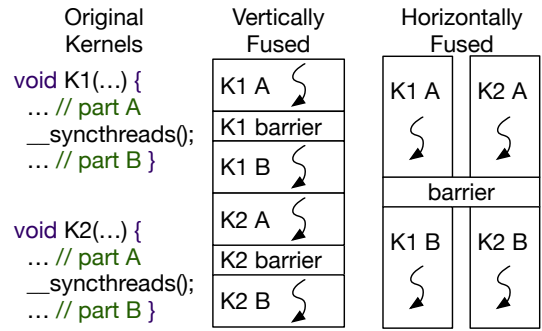


Fig. 1: Vertical and horizontal kernel fusion.

We then evaluate HFUSE at Section IV. Section V discusses related work and Section VI concludes this paper.

II. OVERVIEW

We first introduce background information of GPU architectures that are important for understanding kernel fusion. We next present an overview of two kernel fusion techniques, the standard vertical fusion and our horizontal fusion. We then present an motivating example of applying horizontal fusion with HFUSE. In this paper we use the terminology of NVIDIA CUDA platform [1] and the architecture parameters of NVIDIA Pascal [19] and Volta [20] GPUs. Note that most of the discussed concepts are generally applicable to other GPU platforms and architectures.

A. Background

Kernels, Blocks, and Threads: Kernels are standalone computational routines that the CUDA runtime will dispatch to NVIDIA GPUs to execute in parallel. They are C-like programs that utilize GPU resources including registers, local shared caches, and the global GPU memory. GPUs are SIMD processors, so each kernel launch will start multiple *blocks* in parallel and each block contains multiple threads. The *grid dimension* (i.e., the number of blocks) and the *block dimension* (i.e., the number of threads) are typically tunable constants. It is a common practice in GPU programming to develop kernels that can work with different block dimension parameters. This means that changing block dimensions of the kernels often only influences performance. A kernel program can access its own block id (e.g., `blockIdx.x`) and thread id (e.g., `threadIdx.x`) at the runtime to enable its different threads to potentially process different data.

Stream Multiprocessor and Occupancy: When the CUDA runtime dispatches a kernel to a GPU, the GPU eventually dispatches the blocks of the kernel to Stream Multiprocessors (SMs) to execute. Each GPU has multiple SMs depending on its hardware specification. In the Pascal and Volta architectures, each SM has 64K registers and 96K shared memory cache; each SM can host a maximum of 2048 different threads at the same time; each SM also has multiple CUDA cores for arithmetic operations and multiple memory controllers for accessing the global GPU memory.

Because each SM has the fixed amount of resources, it can execute only a limited amount of blocks in parallel, depending on the kernel resource requirement. This is called the *occupancy* of a kernel. Generally speaking, higher occupancy is usually better because it enables the kernel to exploit the *block-level* parallelism. For example, if a kernel block that uses 24K shared memory, 512 threads, and 64 registers per thread, a SM can only execute two blocks in parallel and the registers become the bottleneck. If the developer optimized the kernel block to use only 32 register per thread, then the SM can now execute four blocks and the developer doubles the occupancy.

Warps, Warp Scheduler, and Instruction Latency: In SMs, each 32 consecutive threads form a warp. Threads inside a warp always execute together in a lock-step fashion and warps are minimum scheduling units in SMs.² The warp scheduler in a SM will select eligible warps to execute — a warp is eligible if 1) all data required for its next instruction is ready, 2) there are idle hardware resources to execute its next instruction (e.g., idle memory controllers for memory access instructions), and 3) it is not stalled by barriers.

Because each SM typically has tens of warps executing in parallel, the warp scheduler may effectively hide *instruction latencies*. If there is a time-consuming instruction in one warp blocking its execution, warp scheduler can switch the SM to execute other eligible warps while waiting for the results of the instruction. Therefore having instructions requesting different hardware resources in a kernel is beneficial because it tends to increase the number of eligible warps for the scheduler. It reduces the chance that the SM execution is completely stalled by instruction latencies.

Synchronization Barriers: The built-in function `__syncthreads()` in CUDA corresponds to block-wide synchronization barriers. It is the main way for threads inside a kernel block to coordinate with each other. An SM will stall the thread execution inside a block at a block-wide barrier until all threads in the block reaches the barrier. Note that barriers may significantly limit the capability of warp schedulers in SMs of hiding instruction latencies, because the schedulers cannot interleave instructions across the barriers.

B. Kernel Fusion

Vertical Kernel Fusion: The standard kernel fusion in deep learning frameworks fuses kernels vertically shown as Figure 1. Suppose we have two kernels `K1()` and `K2()` and both of the kernels have the grid dimension of 512 and the block dimension of 512. The code of the vertically fused kernel will combine the source code of `K1()` and `K2()` in order. Therefore the fused kernel will also has the same grid and block dimensions, but one thread in the fused kernel will execute the instructions of two original threads, one in `K1()` and one in `K2()`. The middle part of Figure 1 shows the execution flow of one thread in the fused kernel.

The major potential performance advantage of the vertical fusion comes from eliminating global memory accesses for

²In the Volta and Turing architectures, warps do not restrictively execute in the lock-step fashion but warps are still the minimum scheduling units

```

1 void batch_norm_collect_statistics(input, isize, output) {
2   __shared__ int shared_n[2 * 2 * WARP_SIZE + WARP_SIZE];
3   ... // Local variable declarations
4
5   // PART A: Compute the mean and variance across (batch, x)
6   // It uses shuffles to partially aggregate the results
7   shared_avg_var = (float*) &shared_n[WARP_SIZE];
8   plane = blockIdx.x; N = isize[0] * isize[2];
9   tid = threadIdx.x + threadIdx.y * blockDim.x;
10  avg = 0; var_n = 0; n = 0;
11  for (int batch = threadIdx.y; batch < isize[0]; batch +=
12    ↳ blockDim.y) {
13    for (int x = threadIdx.x; x < isize[2]; x += blockDim.x)
14      ↳ {
15      float v = input[batch][plane][x];
16      float dl = v - avg;
17      n++; avg += dl / n; var_n += dl * (v - avg); } }
18  for (int i = 0; i < getMSB(WARP_SIZE); ++i) {
19    float o_avg = WARP_SHFL_XOR(avg, 1 << i, WARP_SIZE);
20    int o_n = WARP_SHFL_XOR(n, 1 << i, WARP_SIZE);
21    float factor = 1.0 / fmaxf(1.0, n+o_n);
22    var_n += WARP_SHFL_XOR(var_n, 1 << i, WARP_SIZE) +
23      (avg - o_avg) * (avg - o_avg) * n * o_n *
24      ↳ factor;
25    avg = (n * avg + o_n * o_avg) * factor; n += o_n; }
26  __syncthreads();
27
28  // PART B: Write partially aggregated results to shared
29  ↳ mem
30  if (tid % WARP_SIZE == 0) {
31    shared_n[tid / WARP_SIZE] = n;
32    shared_avg_var[tid / WARP_SIZE * 2] = avg;
33    shared_avg_var[tid / WARP_SIZE * 2 + 1] = var_n; }
34  __syncthreads();
35
36  // PART C: Another round of shuffles to finalize the
37  ↳ results
38  if (tid < WARP_SIZE) {
39    n = (tid < blockDim.x * blockDim.y / WARP_SIZE ?
40      ↳ shared_n[tid] : 0);
41    avg = (tid < blockDim.x * blockDim.y / WARP_SIZE ?
42      ↳ shared_avg_var[2 * tid] : float(0));
43    var_n = (tid < blockDim.x * blockDim.y / WARP_SIZE ?
44      ↳ shared_avg_var[2 * tid + 1] : float(0)); }
45  for (int i = 0; i < getMSB(WARP_SIZE); ++i) {
46    float o_avg = WARP_SHFL_XOR(avg, 1 << i, WARP_SIZE);
47    int o_n = WARP_SHFL_XOR(n, 1 << i, WARP_SIZE);
48    float factor = 1.0 / fmaxf(1.0, n+o_n);
49    var_n += WARP_SHFL_XOR(var_n, 1 << i, WARP_SIZE) +
50      (avg - o_avg) * (avg - o_avg) * n * o_n *
51      ↳ factor;
52    avg = (n * avg + o_n * o_avg) * factor; n += o_n; }
53  if (tid == 0) {
54    ... // Write results to output
55  } }

```

Fig. 2: Normalization kernel.

intermediate results. In this example, the instructions from `K2()` may directly access the output of `K1()` without using expensive global memory read instructions. If some output of `K1()` is only used by `K2()`, the fused kernel can even eliminate associated global memory write instructions. Therefore deep learning frameworks typically apply vertical fusion on neighboring kernels in data dependency graphs.

Note that the vertical fusion may sometime facilitate the instruction interleaving to hide latency, but such effect is typically minimum due to the presence of synchronization barriers. The vertically fused kernel will have as many synchronization barriers as the two original kernels and the warp scheduler cannot interleave instructions across these barriers.

Horizontal Kernel Fusion: Unlike the standard kernel fusion, our horizontal fusion technique creates separate threads for

```

1 __global__ void kernelHistogram1D(TensorInfo a,
  ↪ TensorInfo b, nbins, minvalue, maxvalue,
  ↪ totalElements, getOp) {
2   extern __shared__ unsigned char my_smem[];
3   output_t* smem;
4
5   // PART A: Initialize shared memory counters
6   smem = reinterpret_cast<output_t*>(my_smem);
7   for (int i = threadIdx.x; i < a.sizes[0];
8       i += blockDim.x) { smem[i] = 0; }
9   __syncthreads();
10
11  // PART B: Go over the input b to increment shared
  ↪ counters
12  FOR_KERNEL_LOOP(linearIndex, totalElements) {
13      const int bOffset =
14          ↪ IndexToOffset::get(linearIndex, b);
15      const input_t bVal = b.data[bOffset];
16      if (bVal >= minvalue && bVal <= maxvalue) {
17          const int bin = getBin(bVal, minvalue,
18              ↪ maxvalue, nbins);
19          atomicAdd(&smem[bin], getOp(linearIndex)); } }
20  __syncthreads();
21
22  // PART C: Increment the output a with the shared
  ↪ counters
23  for (int i = threadIdx.x; i < a.sizes[0]; i +=
24      ↪ blockDim.x){
25      const IndexType aOffset =
26          ↪ IndexToOffset<output_t, IndexType,
27              ↪ ADims>::get(i, a);
28      atomicAdd(&a.data[aOffset], smem[i]);
29  } }

```

```

1 void fused_kernel(...) {
2   // Prologue of the fused kernel
3   int global_tid = threadIdx.x + threadIdx.y *
  ↪ blockDim.x + threadIdx.z * BlockDim.x *
  ↪ blockDim.y;
4   int threadIdx_x, threadIdx_y, threadIdx_z;
5   int blockDim_x, blockDim_y, blockDim_z;
6   if (global_tid < 896) {
7       blockDim_x = 896 / 16;
8       blockDim_y = 16; blockDim_z = 1;
9       threadIdx_x = global_tid % blockDim_x;
10      threadIdx_y = global_tid / blockDim_x %
  ↪ blockDim_y;
11      threadIdx_z = 1; i
12  } else {
13      blockDim_x = 128;
14      blockDim_y = 1; blockDim_z = 1;
15      threadIdx_x = (global_tid - 896) % blockDim_x;
16      threadIdx_y = 1; threadIdx_z = 1;
17  }
18  // Variable decls for
  ↪ batch_norm_collect_statistics()
19  __shared__ int shared_n[2 * 2 * WARP_SIZE +
  ↪ WARP_SIZE];
20  ...
21  // Variable decls for kernelHistogram1D()
22  extern __shared__ unsigned char my_smem[];
23  output_t* smem;
24
25  if (!(global_tid < 896)) goto K1_end;
26  // batch_norm_collect_statistics() PART A
27  ...
28  // A PTX assembly to only sync 896 threads.
29  asm("bar.sync 1, 896;");
30  // batch_norm_collect_statistics() PART B
31  ...
32  asm("bar.sync 1, 896;");
33  // batch_norm_collect_statistics() PART C
34  ...
35  K1_end:
36  if (global_tid < 896) goto K2_end;
37  // kernelHistogram1D() PART A
38  smem = reinterpret_cast<output_t*>(my_smem);
39  for (int i = threadIdx_x; i < a.sizes[0];
40      i += blockDim_x) { smem[i] = 0; }
41  // A PTX assembly to only sync 128 threads.
42  asm("bar.sync 2, 128;");
43  // kernelHistogram1D() PART B
44  ...
45  asm("bar.sync 2, 128;");
46  // kernelHistogram1D() PART C
47  ...
48  K2_end:
49  }

```

Fig. 3: Histogram kernel.

instructions of different kernels. The right part of Figure 1 presents the execution flow of the horizontally fused kernel. The fused kernel has the grid dimension of 512 and the block dimension of 1024. The first 512 threads correspond to threads for instructions of K1 () and the remaining threads correspond to K2 (). The fused kernel uses branch statements to check the current thread id to dispatch the thread to execute the corresponding instructions.

Note that it is possible to partition the thread space of a block unevenly in the fused kernel, e.g., assigning one kernel 768 threads and another kernel 256 threads. If the block dimensions of the two original kernels are tunable, there will be multiple ways to fuse the two kernels with different thread space partition schemes. Which one runs fastest typically depends on the workload of the original two kernels.

Hypothesis of Horizontal Fusion: Our hypothesis of the horizontal fusion is that its thread-level parallelism will enable the warp scheduler to interleave instructions from different kernels to hide instruction latencies. It may increase the average eligible warps on SMs to improve the overall performance. If our hypothesis is true, then the horizontal fusion will be mostly beneficial for fusing kernels that use different kinds of instructions and kernels that are memory intensive (because memory instructions have long latencies). Our experimental results in Section IV validate our hypothesis.

C. Motivating Example

Fig. 4: HFUSE fused kernel.

We next present an example of using HFUSE to horizontally fuse two deep learning kernels. Figure 2 shows the simplified code snippet of `batch_norm_collect_statistics()`, a CUDA kernel that computes the mean and variance of an input tensor for normalization. We extracted this kernel source code from the PyTorch framework [16] and this kernel is used by ResNet [21]. The kernel in Figure 2 uses intra-warp shuffles [22] to speed up its computation. It can operate with a tunable block dimension size as long as the size is a multiple of 32. Each thread first computes the partial results of the mean and the variance from the corresponding entries of the

tensor with the loop at lines 10-15. The kernel then uses intra-warp operations to aggregate the partial results of each warp (consecutive 32 threads) at lines 16-22. It then writes the partially aggregated results of the 16 warps to the shared memory at lines 26-29 and further aggregates these partial results to produce the output at lines 33-46.

Figure 3 shows the simplified code snippet of `kernelHistogram1D()`, a tensor analysis kernel in PyTorch to generate histograms over values in an input tensor. Because investigating tensor value distributions at hidden layers is a common practice for developers to tune model parameters, this kernel could be invoked during the training of the ResNet model together with the kernel in Figure 2. `kernelHistogram1D()` uses the shared memory array `my_smem` at lines 2-3 to count the appearances of tensor values in different ranges. This kernel also operates a tunable block dimension size. It initializes the shared counters at lines 6-9. It then iterates the tensor values to atomically increment the shared counters at lines 12-17 and finally merges the shared counter results with the global counter output at lines 21-25.

Given the two kernels in Figures 2 and 3 as the input, HFUSE horizontally combines them to generate a faster fused kernel shown as Figure 4 with the following steps.

Generate Prologue: HFUSE first generates the prologue for the fused kernel shown as lines 2-23 in Figure 4. The fused kernel has 1024 threads per block. The first 896 threads correspond to the first input kernel (e.g., `batch_norm_collect_statistics()`), while the remaining 128 threads correspond to the second input kernel (e.g., `kernelHistogram1D()`). The prologue checks the current thread id and maps it back to the thread ids of the original kernels, storing them into the variables `threadIdx_x`, `threadIdx_y`, and `threadIdx_z`. It also sets variables like `blockDim_x` to the original input kernel dimensions. The prologue finally will include all variable declarations from the two input kernels. HFUSE properly renames these local variables to make sure each of them has a fresh name.

Transform Original Kernels: HFUSE then transforms the original two kernels. Lines 37-40 in Figure 4 present the translated code of the first part of `kernelHistogram1D()`. HFUSE replaces the built-in special values with the corresponding defined variables in the prologue (e.g., replaces `threadIdx.x` with `threadIdx_x` and `blockDim.x` with `blockDim_x`). HFUSE then add additional branch statements to check the current thread id at lines 25 and 36. The branches will skip the execution of the statements of one kernel if the current thread is in the thread range of the other kernel.

Replace Synchronization Barriers: `__syncthreads()` will break the original kernel semantics in the fused kernel, because it will attempt to synchronization all threads in the fused kernel, which include threads for both of the original kernels. To preserve the original kernel semantics, HFUSE replaces synchronization barriers in the original kernels with inlined PTX assembly `bar.sync` instructions at lines 29, 32, 42, and 45 in Figure 4. Note that the second parameter of

`bar.sync` denotes the number of threads participating the barrier [23]. HFUSE passes 896 for this parameter at lines 29 and 32 and passes 128 at lines 42 and 45. Combining with the inserted branch statements at lines 25 and 36, these `bar.sync` instructions will create the desired partial barriers that only synchronize threads within the corresponding thread ranges of each original kernel.

Profile Different Configurations: Because both of the two original kernels support tunable block dimensions, there are multiple ways to partition the thread space of the fused kernel. For example, it is possible to partition the thread space evenly among two kernels. Additionally, the fused kernel will use more registers than any of the two input kernels and high register usage may lower the occupancy. Enforcing a register bound in CUDA may improve the performance of the fused kernel.

HFUSE automatically profiles possible configuration combinations. For Pascal 1080Ti GPU and the default workload of these two original kernels in our experiments, HFUSE outputs the kernel in Figure 4 as the fastest fused kernel and restricts the register usage to 32 per thread. The kernel in Figure 4 runs 53.4% faster than individually executing two kernels in Figures 2 and 3 on 1080Ti. For Volta V100 GPU, the fastest fused kernel partitions the thread space differently. It assigns 768 threads instead of 896 threads for the first kernel and the remaining 256 threads to the second kernel. It runs 15.8% faster than individually executing two kernels on V100.

III. DESIGN

We next present the design of HFUSE. In this section, we represent a kernel as a list of CUDA statements. Macros are preprocessed, function calls are all inlined, and local variable declarations are lifted to the top of the function. We will discuss these preprocessing steps in Section III-C. In pseudo-codes, we use double quotations to denote CUDA statements. For simplicity, in this section we assume that the CUDA kernels have only one block sub-dimension, i.e., `blockDim.y` and `blockDim.z` are one. It is straightforward to extend our algorithm to cover kernels with more than one block sub-dimensions.

A. Generate Fused Kernel

Figure 5 presents the pseudo-code of `Generate()`. Given two input kernels K_1 and K_2 together with their block dimensions d_1 and d_2 , `Generate()` returns the horizontally fused kernel F .

Generate Prologue: The pseudo-code in Figure 5 first copies the local variable declarations from the two input kernels to the fused kernels at line 2. It properly renames them to make sure that the local variables do not have conflict names. At line 3 the pseudo-code defines and initializes a set of special variables, `tid_1` and `tid_2` for storing the original thread id of the two input kernels as well as `size_1` and `size_2` for storing the original block dimension of the two kernels.

Replace Built-in Variables: The pseudo-code at lines 4 then replaces “`threadIdx.x`” and “`blockDim.x`” with the corresponding defined variables in the prologue. This is because

Input : K_1 and K_2 are two input kernels. d_1 and d_2 are the block dimensions of K_1 and K_2 .

Output: A fused kernel F

- 1 **function** *Generate*(K_1, K_2, d_1, d_2) :
- 2 Initialize F with local variable declarations from K_1 and K_2 and extract non declaration statements as S_1 and S_2 .
- 3 Append “tid=threadIdx.x; tid_1=threadIdx.x; tid_2=threadIdx.x- d_1 ; size_1= d_1 ; size_2= d_2 ;” to F
- 4 Replace “threadIdx.x” and “blockDim.x” in S_1 and S_2 with “tid_1” and “size_1” or “tid_2” and “size_2” accordingly.
- 5 Replace “__syncthreads()” in S_1 with the inlined PTX “bar.sync 1, d_1 ;”
- 6 Replace “__syncthreads()” in S_2 with the inlined PTX “bar.sync 2, d_2 ;”
- 7 Append “if (threadIdx.x >= d_1) goto l_1 ;” to F
- 8 Mark the end of S_1 with the label l_1
- 9 Append S_1 to F
- 10 Append “if (threadIdx.x < d_1) goto l_2 ;” to F
- 11 Mark the end of S_2 with the label l_2
- 12 Append S_2 to F
- 13 **return** F

Fig. 5: An algorithm generates the fused kernel.

in the fused kernel, these built-in values will refer to the fused kernel not the original kernel. This replacement preserves the semantics of the statements in the original kernels.

Replace Synchronization Barriers: `__syncthreads()` in CUDA implements a barrier for all threads in a block. In the fused kernel, the instructions from the two input kernels are running concurrently in different threads of a block, so HFUSE needs to replace `__syncthreads()` with partial barriers only for the threads of the corresponding input kernel.

Fortunately, the inlined PTX instruction `bar.sync` can support partial barrier [23]. The first parameter of `bar.sync` is a constant from 0 to 15 denoting the barrier id. The second parameter of `bar.sync` is a constant denoting the number of threads participating the barrier. Internally, the GPU hardware maintains a counter to track how many threads have reached the barrier. When sufficient threads have reached the barrier, they are allowed to progress. The pseudo-code at lines 5-6 replaces `__syncthreads()` with `bar.sync` PTX instructions. These instructions pass the barrier id one for barriers in the first original kernel and two for barriers in the second kernel. They also pass the original block dimension as the second parameter to implement the desired partial barriers. When combined with the branch guards inserted at lines 7 and 10, these `bar.sync` instructions will only wait for threads from their own original kernels instead of for all threads. The fused kernel therefore has synchronization barriers at equivalent places for the equivalent sets of threads as the original two kernels.

Append Guarded Statements: The pseudo-code finally appends the translated statements of two input kernels into the

Input : K_1 and K_2 are two different kernels. d_0 is the desired block dimension of the fused kernel.

Output: A fused kernel F^* and the register bound r^* for launching the kernel.

- 1 **function** *Main*(K_1, K_2, d_0) :
- 2 $t^* \leftarrow \infty$
- 3 $F^* \leftarrow \emptyset$
- 4 $r^* \leftarrow \perp$
- 5 $d_1 \leftarrow 128$
- 6 **while** $d_1 < d_0$ **do**
- 7 $F \leftarrow \text{Generate}(K_1, K_2, d_1, d_0 - d_1)$
- 8 $t \leftarrow \text{Profile the running time of } F$
- 9 **if** $t < t^*$ **then**
- 10 $t^* \leftarrow t$
- 11 $F^* \leftarrow F$
- 12 $r^* \leftarrow \perp$
- 13 $b_1 \leftarrow \frac{\text{SMNRegs}}{d_1 * \text{NRegs}(S_1)}$
- 14 $b_2 \leftarrow \frac{\text{SMNRegs}}{d_2 * \text{NRegs}(S_2)}$
- 15 $b_0 \leftarrow \min(\min(b_1, b_2), \frac{\text{SMShMem}}{\text{ShMem}(F)}, \frac{\text{SMNThreads}}{d_0})$
- 16 $r_0 \leftarrow \frac{\text{SMNRegs}}{b_0 * d_0}$
- 17 $t \leftarrow \text{Profile } F$ with the register bound r_0
- 18 **if** $t < t^*$ **then**
- 19 $t^* \leftarrow t$
- 20 $F^* \leftarrow F$
- 21 $r^* \leftarrow r_0$
- 22 $d_1 \leftarrow d_1 + 128$
- 23 **return** F^*, r^*

Fig. 6: A search algorithm finds the best fusion configuration.

fused kernel at lines 7-12. Before appending the statements of each kernel, HFUSE will insert an if statement to check the current thread index at lines 7 and 10. In the fused kernel, the threads in the index range of $[0, d_1)$ correspond to the first input kernel, while the threads in the index range of $[d_1, d_1 + d_2)$ correspond to the second input kernel. If the index is outside the range of the corresponding input kernel, it will skip the statements from the kernel.

B. Search Fusion Configuration

Figure 6 presents the pseudo-code of our main algorithm to search for the best fusion configuration. Given statements from two kernels S_1 and S_2 and the desired block dimension of the fused kernel d_0 , the algorithm produces a horizontally fused kernel kernel F^* as its output.

Thread Space Partition: The pseudo-code uses a loop at lines 6-22 to search for the best thread space partition. At each iteration, it tries a different block dimension for the first kernel (i.e., d_1), generates the fused kernel at line 7, and profiles the running time of the fused kernel twice, once without any register bound at line 8 and once with a calculated register bound at line 17. At lines 10-12 and 19-21, the pseudo-code records the fastest fused kernel together with its configuration.

Note that HFUSE searches the block dimension of the first kernel at a granularity of 128, because using an irregular block dimension often breaks memory access patterns and causes CUDA kernels to run slower.

Limit Register Usage for Occupancy: The fused kernel may require more registers than each of the original two kernels. This additional register requirement may lower the occupancy, each SM will be able to execute less blocks concurrently due to the available total registers per SM. In practice, the CUDA compiler can enforce a bound to limit the number of registers used in a compiled kernel. Excessive registers will be spilled into the global GPU memory. It is therefore possible to recover the occupancy loss at the cost of introducing expensive memory instructions.

The pseudo-code in Figure 6 automatically explores this trade-off with profiling. For each different thread space partition, HFUSE will attempt to compile the fused kernel twice with different configurations, one without the register bound and one with it. When the algorithm sets the bound, it computes the bound r_0 at lines 13-16. Note that SMNRegs is the number of registers per SM (64K for Pascal and Volta GPUs), SMSMem is the shared memory size per SM (96K for Pascal and Volta GPUs), SMNThreads is the maximum number of concurrent threads per SM (2048 for Pascal and Volta GPUs), b_1 and b_2 are the numbers of concurrent active block while launching the original two kernels, ShMem() denotes the used shared memory size of a kernel, and NRegs() denotes the number of used registers of a kernel. The intuition of this bound is to make the fused kernel to run as many blocks per SM as the two input kernels, unless the occupancy is otherwise bounded by the number of threads or the shared memory usage.

C. Implementation

We implemented HFUSE based on the front-end CUDA parser of the LLVM Clang framework [24]. The front-end parser converts the CUDA source code into abstract syntax trees (ASTs) and HFUSE traverses ASTs to implement the algorithm we described in Section III. For each input kernel file, our implementation uses Clang to pre-process all macros and included headers. We also use the built-in functionalities from the Clang front-end to inline all function calls in the input kernels. HFUSE does not support recursive function calls. Note that recursion is extremely rare in GPU kernels, because GPUs are very inefficient at handling it as well. In our experiments, we do not encounter any kernel that contains recursive calls.

Additionally, HFUSE traverses the AST of the input kernel to locate all local variable declarations. It renames each local variable to make sure that they will not cause name conflicts in the fused kernel. It also lifts their declarations to the start of the kernel. If the declaration of a local variable is associated with initialization assignments, it will still lift the declaration but create corresponding new assignment statements at the original location of the declaration. HFUSE lifts local variable declarations because it instruments goto statements into the

fused kernel and CUDA may not allow goto statements to jump over local variable declarations.

IV. EXPERIMENTAL RESULTS

We next evaluate HFUSE with 5 deep learning computational kernels and 4 cryptography computational kernels. The goal of this evaluation is to answer the following questions:

- How effective is HFUSE? How do the horizontally fused kernels compare with native kernels and the vertically fused kernels in performance?
- Why do the horizontal fused kernels run faster?
- What is the right scenario to apply the horizontal fusion?
- How much improvement does the automatic profiling technique have on fusing kernels with barriers?

A. Methodology

Benchmark Kernels: We collect 9 GPU kernels including 5 deep learning computational kernels and 4 cryptography computational kernels: Maxpool applies a 2D maxpooling over an input matrix; Batchnorm collects the batch mean and variance a 2D input matrix, which will then be used for normalization; Upsample applies a 2D bilinear upsampling over a input matrix; Im2Col rearranges the input image blocks into columns; Hist computes the histogram of an input matrix. These kernels have been widely used in AI models such as ResNet [21], BigGAN [25], and UVC [26]. Ethash is a memory intensive hash function used by Ethereum [27] for its proof of work mining. SHA256, Blake256, and Blake2B are three computational intensive hash functions used for the proof-of-work of several cryptocurrencies.

All deep learning computational kernels are extracted from PyTorch [16]. Ethash is extracted from ethminer [17], and the rest three cryptography computational kernels are collected from ccmminer [18]. The 5 deep learning kernels form 10 possible benchmark pairs, while the 4 crypto kernels form 6 possible benchmark pairs. Note that all deep learning kernels support tunable block dimensions while crypto kernels do not.

Apply HFUSE: For each benchmark pair, we apply HFUSE to horizontally fuse the two kernels. We run the fused kernel and measure its running time. For comparison, we measure the running time of launching the original kernels individually via parallel CUDA streams. We implement the standard vertical fusion and compares its running time with HFUSE as well. To evaluate the effect of our profiling techniques, we also run a version of HFUSE that evenly partition the thread space for two kernels without profiling. Note that because crypto kernels do not support tunable block dimensions, HFUSE always evenly partition the space instead. We use nvprof, a profiling tool provided by CUDA toolkit, to collect the performance data of each kernel. In all experiments we take into account two generations of NVIDIA GPU cards: GeForce GTX 1080 Ti graphic card based on Pascal, and Tesla V100 graphic card based on Volta.

Run Different Workload: All benchmark kernels can operate with variable workload. Deep learning kernels can process inputs with different sizes, while cryptography kernels can run

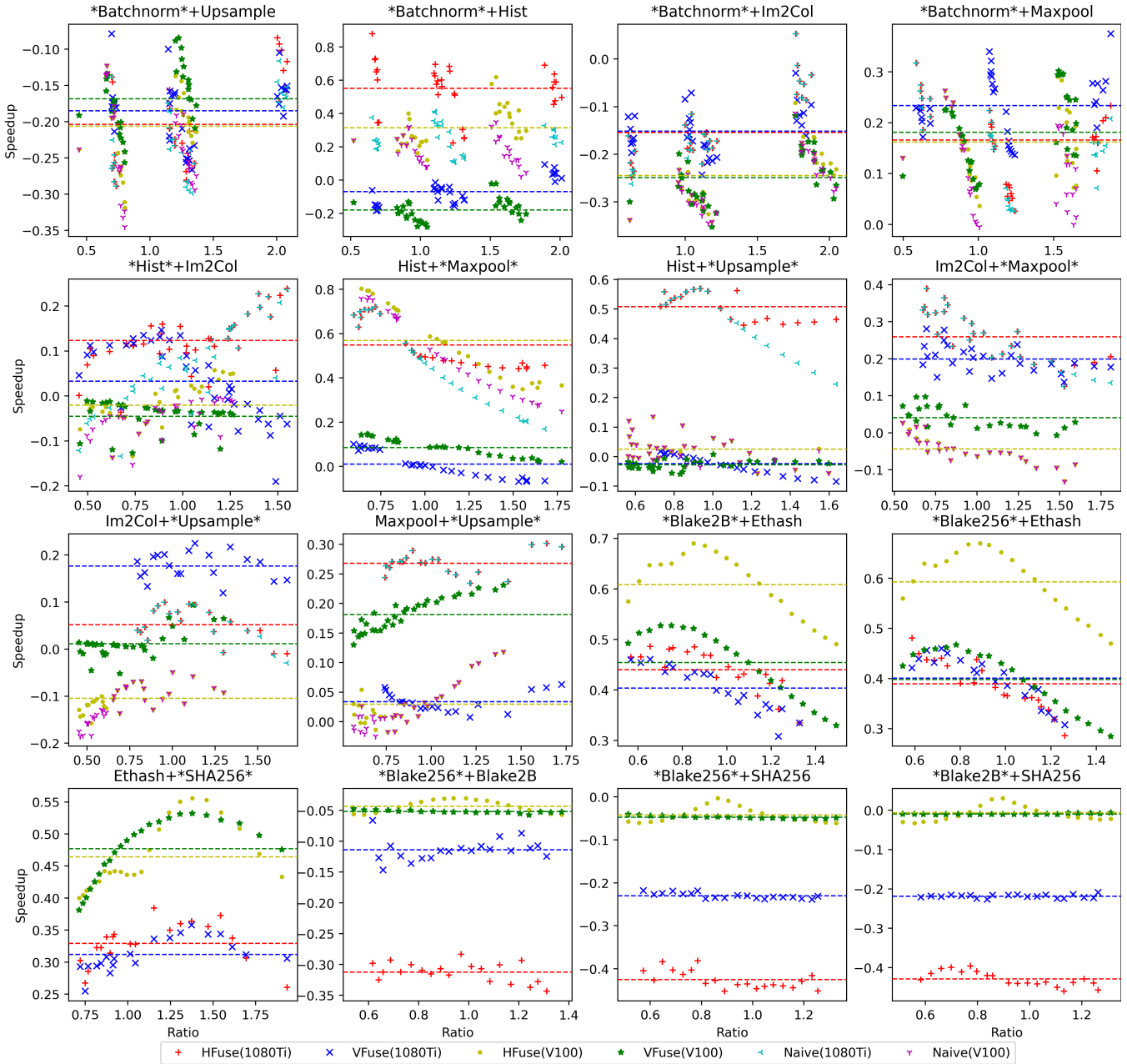


Fig. 7: Kernel execution time speedup.

iterations to compute multiple hashes. The speed up of any fusion technique depends on the execution time ratio of two input kernels, i.e., fusing two kernels with similar execution time will be typically more beneficial. To understand how horizontal fusion works in different workload ratio, we run our experiments with different input sizes for each kernel. For each benchmark pair, we will report the speed up under different execution time ratios of the two original kernels.

Execution Time Measurement: Since it may take a while for the GPU performance to stabilize, we launch a dummy kernel on the GPU for about 500 millisecond before launching any experimental kernels. For each pair of kernels, we record

elapsed time after the first kernel launches and before the second kernel finishes with nvprof as the native execution time.

Performance Analysis: For each benchmark kernel, we select a representative input size so that the execution time ratios of the ten benchmark pairs are close to one. To understand the effect of register bounds, we make HFUSE to generate two fused kernels, with and without register bounds. For each variant of the fused kernels under the representative input size, we use nvprof to collect four metrics besides its execution time:

Kernel	Execution Time (ms)	Issue Slot Utilization (%)	MemInst Stall (%)	Occupancy (%)
Im2Col	1.92 / 1.69	87.18 / 63.81	27.5 / 38.2	48.0 / 48.1
Maxpool	1.93 / 1.97	7.99 / 8.55	95.2 / 97.2	89.5 / 92.2
Upsample	1.72 / 2.41	34.32 / 23.29	77.8 / 81.3	48.3 / 49.7
Hist	1.70 / 1.90	14.46 / 50.70	1.4 / 7.3	99.0 / 74.3
Batchnorm	2.15 / 1.90	61.83 / 63.27	52.2 / 60.3	96.2 / 98.1
Blake256	38.43 / 37.33	91.01 / 53.22	1.3 / 0.0	48.9 / 48.9
Blake2B	39.20 / 39.40	90.15 / 52.44	1.7 / 0.0	49.1 / 48.9
SHA256	42.88 / 39.69	65.62 / 49.07	0.0 / 0.0	30.6 / 24.6
Ethash	46.01 / 37.23	10.88 / 4.17	96.1 / 96.6	36.7 / 18.2

Fig. 8: Metrics of individual kernels.

- **Issue Slot Utilization:** Percentage of issue slots that issued at least one instruction. The streaming multiprocessor is stalled because of instruction latencies.
- **MemInst Stall:** Percentage of stalls caused by waiting for memory instructions.
- **Occupancy:** Ratio of the average active wraps per active cycle to the theoretically number of warps supported on a multiprocessor.
- **Elapsed Cycles:** Elapsed clocks of the launched kernel.

We also computes the average issue slot utilization while executing two native kernels using the following formula:

$$I_{k_1+k_2} = \frac{I_{k_1} * C_{k_1} + I_{k_2} * C_{k_2}}{C_{k_1} + C_{k_2}}$$

where I_k and C_k are the issue slot utilization and the elapsed cycles of kernel k .

B. Performance Results

Figure 7 shows the kernel execution time speedup with respect to the native execution of 16 pairs of kenels. In each subplot, the x-axis represents the ratios of execution time of two kernels; the y-axis represents the speedup of the fused kernel with resepect to the native execution. Each subplot has four kinds of markers which represent standard fusion (VFuse) and horizontal fusion (HFuse) on two different GPU generations (1080Ti and V100). For deep learning kernels, we also include two additional kinds of markers to represent horizontal fusion without thread space profiling (Naive) on the two GPU generations.

For each benchmark pair, we change the input size of one benchmark kernel (marked with “*” in the pair name in Figure 7) to obtain results on different execution time ratios of the two kernels. Different marks of the same kind correspond to experimental results of different input sizes. Each subplot in Figure 7 also draws four horizontal lines in the corresponding color to represent the average speedup of the fused kernel across different execution ratio data points. Note that the execution time of Batchnorm changes non-continuously as its input size changes, so the marks in the four pairs involving Batchnorm appear in clusters.

Our results highlight the effectiveness of our automatic horizontal fusion technique across two different domains. For 5 out of the 10 deep learning cases (*Batchnorm*+Hist,

Batchnorm+Maxpool, Hist+*Maxpool*, Hist+*Upsample*, and Maxpool+*Upsample*) and for 3 out of the 6 crypto cases (pairs with Ethash), the HFUSE fused kernel outperforms the native execution across different execution time ratios on both 1080Ti and V100. For these cases, the HFUSE marks are almost always on the positive side of the y-axis. The average speedup of HFUSE over different execution time ratios on these 9 cases are 12.4%-55.1% on 1080Ti and 2.5%-60.8% on V100. For 8 cases on 1080Ti and 5 cases on V100 (out of the total 16 cases), the HFUSE fused kernel on average over different execution time ratios outperforms both the standard fusion and the native execution.

We observe that the HFUSE fused kernels have more significant speedup on those cases where one of the original kernels is memory intensive. This is because the horizontal fusion interleaves memory instructions of such a kernel with other instructions to hide latencies of these expensive memory instructions. Note that both kernel fusion techniques perform badly on *Blake256*+Blake2B, *Blake256*+SHA256, and *Blake2B*+SHA256, because those cryptography computational kernels require similar computational resources and fusing such kernels together will bring little benefits but harm the occupancies.

Our results also show the importance of the thread space partition. The automatic profiling technique enables HFUSE to better fuse kernels that have different execution times. For all deep learning cases except *Batchnorm*+Im2Col, the thread space profiling technique is able to find a thread space partition scheme that performs better than the naive approach for some execution time ratio. Better partitioning the thread space will make threads for the two original kernels to co-exist longer so that the warp scheduler can better interleave their instructions.

C. Kernel Metrics Results

To understand in what scenario HFUSE performs best, we collect the performance metrics of the original kernels and the HFUSE fused kernel variants under a representative workload in which the execution time of benchmark kernels is close to each other. Figure 8 shows the results of individual kernels. Each row corresponds to the metrics of one kernel. Figure 9 shows the results of the HFUSE fused kernels. Each entry in Figure 8 and Figure 9 is of the form “X / Y”, where X is the result for 1080Ti GPU and Y is the result for V100

Pairs	Type	Speedup (%)	Issue Slot Utilization (%)		MemInst Stall (%)	Occupancy (%)
			HFUSE	Native		
Batchnorm+Upsample	N-RegCap	-35.0 / -37.4	32.05 / 25.93	52.29 / 41.69	67.2 / 76.1	42.9 / 42.9
	RegCap	-23.4 / -28.9	38.35 / 29.73		75.0 / 80.7	87.1 / 83.2
Batchnorm+Hist	N-RegCap	51.2 / -28.5	55.89 / 33.43	40.55 / 57.22	45.6 / 49.7	90.7 / 43.0
	RegCap	53.4 / 15.8	56.74 / 53.33		46.1 / 56.3	91.1 / 96.0
Batchnorm+Im2Col	N-RegCap	-31.1 / -42.8	44.43 / 31.55	73.65 / 64.81	50.8 / 67.6	37.3 / 42.0
	RegCap	-12.7 / -31.1	58.13 / 41.55		63.4 / 74.5	92.0 / 85.3
Batchnorm+Maxpool	N-RegCap	7.8 / 3.4	32.58 / 28.41	35.73 / 35.28	67.3 / 78.2	64.1 / 72.7
	RegCap	7.8 / 3.4	32.58 / 32.20		67.5 / 78.2	64.0 / 72.7
Hist+Im2Col	N-RegCap	12.2 / -17.3	60.34 / 40.69	51.90 / 58.03	20.0 / 31.6	38.1 / 37.4
	RegCap	11.3 / -0.1	60.09 / 51.32		19.8 / 46.1	38.3 / 78.6
Hist+Maxpool	N-RegCap	52.5 / 56.6	19.07 / 36.25	11.05 / 28.58	26.7 / 43.5	67.5 / 59.0
	RegCap	53.4 / 57.1	19.10 / 39.07		25.0 / 43.0	67.7 / 57.5
Hist+Upsample	N-RegCap	4.4 / -5.7	30.17 / 35.01	26.87 / 35.70	40.8 / 41.2	38.5 / 43.5
	RegCap	51.4 / 5.7	41.20 / 36.37		48.0 / 57.0	77.6 / 82.6
Im2Col+Maxpool	N-RegCap	7.0 / -12.0	51.52 / 30.47	45.95 / 34.05	54.7 / 69.3	32.6 / 32.5
	RegCap	25.3 / -7.5	57.87 / 33.87		62.5 / 74.4	63.5 / 58.4
Im2Col+Upsample	N-RegCap	5.4 / -10.8	71.92 / 36.72	64.76 / 41.11	43.0 / 72.2	42.7 / 44.9
	RegCap	-24.1 / -45.5	49.50 / 24.24		73.6 / 78.9	73.7 / 74.0
Maxpool+Upsample	N-RegCap	-1.6 / -3.4	23.39 / 16.18	22.47 / 17.00	79.3 / 86.4	30.0 / 33.1
	RegCap	29.4 / 1.1	30.32 / 17.97		81.0 / 88.3	60.9 / 62.3
Blake2B+Ethash	N-RegCap	15.9 / 30.1	58.93 / 36.73	47.39 / 28.29	22.8 / 25.5	15.8 / 8.6
	RegCap	42.9 / 65.8	70.08 / 46.85		19.8 / 23.9	29.0 / 29.2
Blake256+Ethash	N-RegCap	17.0 / 30.3	57.89 / 37.05	47.49 / 28.46	19.5 / 26.5	16.1 / 8.6
	RegCap	47.4 / 64.7	71.41 / 46.79		17.6 / 24.7	29.3 / 29.3
Ethash+SHA256	N-RegCap	8.8 / 37.0	39.25 / 36.62	36.97 / 26.81	10.3 / 26.8	15.7 / 8.8
	RegCap	35.1 / 44.1	50.51 / 39.37		18.4 / 16.5	28.8 / 28.8
Blake256+Blake2B	N-RegCap	-26.5 / -2.7	66.08 / 51.34	90.58 / 52.82	2.3 / 0.0	37.5 / 36.8
	RegCap	-96.5 / -96.1	3.60 / 3.31		72.0 / 62.4	98.4 / 96.0
Blake256+SHA256	N-RegCap	-44.3 / -1.0	41.13 / 50.22	77.81 / 51.11	0.9 / 0.0	22.7 / 24.4
	RegCap	-51.2 / -37.4	42.57 / 34.32		43.0 / 7.7	56.2 / 51.6
Blake2B+SHA256	N-RegCap	-42.9 / 2.8	41.40 / 50.26	77.49 / 50.74	0.8 / 0.0	22.7 / 24.5
	RegCap	-50.9 / -31.7	38.27 / 35.30		48.0 / 7.6	54.9 / 50.6

Fig. 9: Metrics of HFUSE fused kernels.

GPU. In order to understand some key factors that influence the performance of the fused kernels. We collect metrics for kernels both with register bound (RegCap) and without register bound (N-RegCap).

The third column in Figure 9 shows the speedup of the fused kernel against the native execution. The fourth column presents the instruction issue slot utilization for the fused kernels and the fifth column presents the average instruction issue slot utilization computed from the metrics of two individual kernels (from Figure 8). The issue slot utilization denotes the percentage of GPU cycles that at least one warp is active for a kernel (that SMs are not stalled due to instruction latencies). The last two columns present the percentages of the stalls caused by memory instructions and the achieved occupancies of the kernels.

Issue Slot Utilization: Our results indicate that HFUSE is effective because horizontal fusion interleaves instructions to hide the instruction latencies. For all cases, a fused kernel runs faster than the native execution if the fused kernel has a higher issue slot utilization. On one hand, the fused kernel will have a much better performance if two kernels uses two different computational resources. For example, Ethash is a memory intensive kernel and Blake256 is a compute intensive kernel. As

shown in Figure 8, the percentage of stalls caused by waiting for memory instructions of Ethash is 96.1% on 1080Ti GPU. The percentage of Blake256 is only 1.3%. Therefore, the issue slot utilization of the fused kernel of Ethash and Blake256 is 23.9% higher than the native execution. The fused kernel hides high latency of the memory instructions in Ethash by interleaving computation instructions from Blake256. On the other hand, fusing two compute-intensive kernels is not very beneficial, as shown by the Blake256+Blake2B, Blake256+SHA256, and Blake2B+SHA256 cases.

Thread-level v.s. Block-level Parallelism: The horizontal fusion may lower the occupancy, which is another key factor that influence the performance. Occupancy indicates the ratio of the average active wraps per active cycle to the theoretically number of wraps supported on a Stream Multiprocessor (SM). If the number of blocks which can execute concurrently on a streaming processor is low, the occupancy of the kernel will also be low because there are not enough eligible warps to be launched. The horizontal fusion may increase the number of registers per thread of the fused kernel, which may limit the maximum number of active blocks on an SM.

Therefore one could view the horizontal fusion as a technique to navigate the inherent trade-off between the thread-

level parallelism of interleaving instructions from more threads and the block-level parallelism of running more blocks per SM. Our results show that it is often beneficial to apply horizontal fusion to gain thread-level parallelism even at the cost of block-level parallelism. For cases including Batch-norm+Maxpool and Hist+Maxpool, the fused kernels have lower occupancies on 1080Ti and V100 GPUs than both of the corresponding original kernels but they run faster.

Register Bound: The register bound may recover the occupancy loss at the cost of additional memory instructions for spilled registers. Our results show that the fused kernel with the register bound may perform better than the kernel without it. For example, Hist+Upsample only achieves 38.5% occupancy without a bound, but it achieves 77.6% occupancy with the bound on 1080Ti GPU. Because of the large improvement of the occupancy, for this case the version with the register bound runs significantly faster. We also noticed that the register bound may cause register spilling and increase the percentage of stalls caused by memory instructions. The MemInst Stall of Im2Col+Upsample is 43.0% on 1080Ti without a bound, and the number increases to 73.6% when the kernel is launched with the bound. Because of the cost of spilled registers, for this case the version without the register bound runs faster. Fortunately, HFUSE automatically profiles two different versions to decide whether to set the register bound or not.

V. RELATED WORK

Kernel Fusion: Wang et al. proposed three different strategies to fusion including concatenating the computation of two kernels similar to the standard vertical fusion, and the distribution of the computation among different threads similar to horizontal fusion [11]. However, their proposed technique cannot handle synchronization barriers and it is not automated. Due to these limitations, their results show that distributing computation among different threads is the worst fusion strategy out of the three proposed fusion strategies. In contrast, our technique do not have these limitations. Our results show that the horizontal fusion, after appropriately handling barriers and automatically profiling the best thread space partition scheme, often outperforms the vertical fusion.

There is a rich set of previous work that targets automatic vertical fusion. Fousek et al. presents a searching technique that finds a linearized kernel with lowest memory requirement [12]. Wahib and Maruyama proposes to formalize kernel fusion as an optimization problem [13]. Springer et al. proposes a new language, called Ikra, for efficient GPU programming that allows a programmer to implement GPU programs of multiple reusable parallel sections [28]. Ikra then fuses those parallel sections into a small number of GPU kernels. Filipovič et al. present a source-to-source compiler that is able to automatically fuse kernels that can be expressed in the form of map and reduce calls [14]. All these prior works only consider vertical fusion, rather than the horizontal fusion proposed in our work.

Kernel Fusion in ML: Kernel fusion is a critical optimization technique for machine learning applications. Appleyard et al. demonstrates several optimization techniques including kernel fusion that can be applied to improve the performance of RNN, GRU, and LSTM models, although they only consider vertical fusion and the optimization can not be automated [9]. Similarly, Diamos et al. presents a framework that fused all the kernels across different time steps into a single kernel [10]. However their main purpose is to keep weight parameters stashed in registers/cache, and enable the training of deeper RNN networks on much larger datasets. Sivathanu et al. proposes a compilation and execution framework that uses measurement-driven approach to guide the compiler to select candidate kernels that can be fused [29].

ML Compilers: Machine learning compiler stack such as TVM [3] and XLA [7] provide an end-to-end solution to speed up both training and inference phases of machine learning models. XLA has been targeting specifically for linear optimization. TVM demonstrates large benefits on mobile platform and IoT devices, but incremental gain on GPU. Wei et al. presents a software stack for machine learning, which uses a linear algebraic IR and generates GPU kernels automatically, although no evaluation results were given regarding its performance [8]. nGraph [6] library is an open-source C++ graph compiler for Deep Learning ecosystems. With nGraph Library, data scientists can use their preferred deep learning framework on any number of hardware architectures. Glow [5] accepts a computation graph from deep learning frameworks, such as PyTorch, and generates highly optimized code for machine learning accelerators. TASO [4] is a deep neural network computation graph optimizer that fuses different matrix operators using graph substitution. Many machine learning compilers employ vertical fusion as their standard fusion technique to save memory operations, but none of previous ML compilers implements automatic horizontal fusion.

Warp Specialization: Singe [30] and CudaDMA [31] use warp specialization techniques to speed up domain-specific applications (e.g., chemistry for Singe and direct memory access library for CudaDMA). Similar to horizontal fusion, the idea of warp specialization is to allow warps in a block to perform different tasks in parallel. Comparing to HFUSE, Singe and CudaDMA have more significant speed up but can only apply to specific domains.

Multi-Application Concurrency: Previous work also proposes techniques to enable better multi-application concurrency [32–35]. These systems modify the GPU runtime and may introduce overhead. KernelMerge [35] modifies the OpenCL runtime to launch and execute two kernels concurrently, which is similar to CUDA stream parallelization. Similarly, Ausavarungnirun et al. suggests to redesign the GPU memory virtualization to mitigate address transaction overhead while supporting multi-application concurrency [36].

VI. CONCLUSION

Automatic horizontal fusion is an effective optimization technique that complements the standard vertical kernel fusion

and it can speedup GPU programs in domains like deep learning and cryptocurrency mining. Our experimental results show that the horizontal fusion can enable warp schedulers in NVIDIA GPUs to interleave instructions from different kernels to hide instruction latencies. It is especially beneficial to apply this technique to fuse kernels with instructions that require different kinds of hardware resources.

REFERENCES

- [1] J. Nickolls, I. Buck, M. Garland, and K. Skadron, "Scalable parallel programming with cuda," *Queue*, vol. 6, no. 2, pp. 40–53, Mar. 2008. [Online]. Available: <http://doi.acm.org/10.1145/1365490.1365500>
- [2] "Mlperf training v0.6 results," <https://mlperf.org/training-results-0-6/>.
- [3] T. Chen, T. Moreau, Z. Jiang, L. Zheng, E. Yan, H. Shen, M. Cowan, L. Wang, Y. Hu, L. Ceze, C. Guestrin, and A. Krishnamurthy, "TVM: An automated end-to-end optimizing compiler for deep learning," in *13th USENIX Symposium on Operating Systems Design and Implementation (OSDI 18)*. Carlsbad, CA: USENIX Association, Oct. 2018, pp. 578–594. [Online]. Available: <https://www.usenix.org/conference/osdi18/presentation/chen>
- [4] Z. Jia, O. Padon, J. Thomas, T. Warszawski, M. Zaharia, and A. Aiken, "Taso: Optimizing deep learning computation with automatic generation of graph substitutions," in *Proceedings of the 27th ACM Symposium on Operating Systems Principles*, ser. SOSP '19. New York, NY, USA: ACM, 2019, pp. 47–62. [Online]. Available: <http://doi.acm.org/10.1145/3341301.3359630>
- [5] N. Rotem, J. Fix, S. Abdulrasool, S. Deng, R. Dzhabarov, J. Hegeman, R. Levenstein, B. Maher, N. Satish, J. Olesen, J. Park, A. Rakhov, and M. Smelyanskiy, "Glow: Graph lowering compiler techniques for neural networks," *CoRR*, vol. abs/1805.00907, 2018. [Online]. Available: <http://arxiv.org/abs/1805.00907>
- [6] F. Boemer, Y. Lao, R. Cammarota, and C. Wierzynski, "ngraph-he: A graph compiler for deep learning on homomorphically encrypted data," in *Proceedings of the 16th ACM International Conference on Computing Frontiers*, ser. CF '19. New York, NY, USA: ACM, 2019, pp. 3–13. [Online]. Available: <http://doi.acm.org/10.1145/3310273.3323047>
- [7] M. Abadi, A. Agarwal, P. Barham, E. Brevdo, Z. Chen, C. Citro, G. S. Corrado, A. Davis, J. Dean, M. Devin, S. Ghemawat, I. Goodfellow, A. Harp, G. Irving, M. Isard, Y. Jia, R. Jozefowicz, L. Kaiser, M. Kudlur, J. Levenberg, D. Mané, R. Monga, S. Moore, D. Murray, C. Olah, M. Schuster, J. Shlens, B. Steiner, I. Sutskever, K. Talwar, P. Tucker, V. Vanhoucke, V. Vasudevan, F. Viégas, O. Vinyals, P. Warden, M. Wattenberg, M. Wicke, Y. Yu, and X. Zheng, "TensorFlow: Large-scale machine learning on heterogeneous systems," 2015, software available from tensorflow.org. [Online]. Available: <https://www.tensorflow.org/>
- [8] R. Wei, V. S. Adve, and L. Schwartz, "Dlvm: A modern compiler infrastructure for deep learning systems," *ArXiv*, vol. abs/1711.03016, 2017.
- [9] J. Appleyard, T. Kociský, and P. Blunsom, "Optimizing performance of recurrent neural networks on gpus," *CoRR*, vol. abs/1604.01946, 2016. [Online]. Available: <http://arxiv.org/abs/1604.01946>
- [10] G. Diamos, S. Sengupta, B. Catanzaro, M. Chrzanowski, A. Coates, E. Elsen, J. Engel, A. Hannun, and S. Satheesh, "Persistent rnn: Stashing recurrent weights on-chip," in *Proceedings of the 33rd International Conference on Machine Learning - Volume 48*, ser. ICML'16. JMLR.org, 2016, pp. 2024–2033. [Online]. Available: <http://dl.acm.org/citation.cfm?id=3045390.3045604>
- [11] G. Wang, Y. Lin, and W. Yi, "Kernel fusion: An effective method for better power efficiency on multithreaded gpu," in *2010 IEEE/ACM Int'l Conference on Green Computing and Communications Int'l Conference on Cyber, Physical and Social Computing*, Dec 2010, pp. 344–350.
- [12] J. Fousek, J. Filipovič, and M. Madzin, "Automatic fusions of cuda-gpu kernels for parallel map," *SIGARCH Comput. Archit. News*, vol. 39, no. 4, pp. 98–99, Dec. 2011. [Online]. Available: <http://doi.acm.org/10.1145/2082156.2082183>
- [13] M. Wahib and N. Maruyama, "Scalable kernel fusion for memory-bound gpu applications," in *SC '14: Proceedings of the International Conference for High Performance Computing, Networking, Storage and Analysis*, Nov 2014, pp. 191–202.
- [14] J. Filipovič, M. Madzin, J. Fousek, and L. Matyska, "Optimizing cuda code by kernel fusion: application on blas," *The Journal of Supercomputing*, vol. 71, no. 10, pp. 3934–3957, Oct 2015. [Online]. Available: <https://doi.org/10.1007/s11227-015-1483-z>
- [15] T. Chen, M. Li, Y. Li, M. Lin, N. Wang, M. Wang, T. Xiao, B. Xu, C. Zhang, and Z. Zhang, "Mxnet: A flexible and efficient machine learning library for heterogeneous distributed systems," *CoRR*, vol. abs/1512.01274, 2015. [Online]. Available: <http://arxiv.org/abs/1512.01274>
- [16] A. Paszke, S. Gross, S. Chintala, G. Chanan, E. Yang, Z. DeVito, Z. Lin, A. Desmaison, L. Antiga, and A. Lerer, "Automatic differentiation in PyTorch," in *NIPS Autodiff Workshop*, 2017.
- [17] "Ethminer, ethereum miner with opencl, cuda and stratum support," <https://github.com/ethereum-mining/ethminer>.
- [18] "ccminer, a cuda accelerated mining application," <https://github.com/tpruvot/ccminer>.
- [19] "Nvidia tesla p100, the most advanced datacenter accelerator ever built," <https://images.nvidia.com/content/pdf/tesla/whitepaper/pascal-architecture-whitepaper.pdf>.

- [20] “Nvidia tesla v100 gpu architecture,” <https://images.nvidia.com/content/volta-architecture/pdf/volta-architecture-whitepaper.pdf>.
- [21] K. He, X. Zhang, S. Ren, and J. Sun, “Deep residual learning for image recognition,” 06 2016, pp. 770–778.
- [22] “Faster parallel reductions on kepler,” <https://devblogs.nvidia.com/faster-parallel-reductions-kepler>.
- [23] “Parallel thread execution isa version 6.5,” <https://docs.nvidia.com/cuda/parallel-thread-execution/index.html>.
- [24] “Clang: a c language family frontend for llvm,” <https://clang.llvm.org/>.
- [25] A. Brock, J. Donahue, and K. Simonyan, “Large scale gan training for high fidelity natural image synthesis,” *ArXiv*, vol. abs/1809.11096, 2018.
- [26] X. Li, S. Liu, S. D. Mello, X. Wang, J. Kautz, and M.-H. Yang, “Joint-task self-supervised learning for temporal correspondence,” in *NeurIPS*, 2019.
- [27] G. Wood, “Ethereum: A secure decentralised generalised transaction ledger,” *Ethereum project yellow paper*, vol. 151, pp. 1–32, 2014.
- [28] M. Springer, P. Wauligmann, and H. Masuhara, “Modular array-based gpu computing in a dynamically-typed language,” in *Proceedings of the 4th ACM SIGPLAN International Workshop on Libraries, Languages, and Compilers for Array Programming*, ser. ARRAY 2017. New York, NY, USA: ACM, 2017, pp. 48–55. [Online]. Available: <http://doi.acm.org/10.1145/3091966.3091974>
- [29] M. Sivathanu, T. Chugh, S. S. Singapuram, and L. Zhou, “Astra: Exploiting predictability to optimize deep learning,” in *Proceedings of the Twenty-Fourth International Conference on Architectural Support for Programming Languages and Operating Systems*, ser. ASPLOS ’19. New York, NY, USA: ACM, 2019, pp. 909–923. [Online]. Available: <http://doi.acm.org/10.1145/3297858.3304072>
- [30] M. Bauer, S. Treichler, and A. Aiken, “Singe: Leveraging warp specialization for high performance on gpus,” in *Proceedings of the 19th ACM SIGPLAN Symposium on Principles and Practice of Parallel Programming*, ser. PPOPP ’14. New York, NY, USA: ACM, 2014, pp. 119–130. [Online]. Available: <http://doi.acm.org/10.1145/2555243.2555258>
- [31] M. Bauer, H. Cook, and B. Khailany, “Cudadma: Optimizing gpu memory bandwidth via warp specialization,” in *SC ’11: Proceedings of 2011 International Conference for High Performance Computing, Networking, Storage and Analysis*, 2011, pp. 1–11.
- [32] S. Pai, M. J. Thazhuthaveetil, and R. Govindarajan, “Improving gpgpu concurrency with elastic kernels,” in *Proceedings of the Eighteenth International Conference on Architectural Support for Programming Languages and Operating Systems*, ser. ASPLOS ’13. New York, NY, USA: ACM, 2013, pp. 407–418. [Online]. Available: <http://doi.acm.org/10.1145/2451116.2451160>
- [33] R. Ausavarungnirun, J. Landgraf, V. Miller, S. Ghose, J. Gandhi, C. J. Rossbach, and O. Mutlu, “Mosaic: A gpu memory manager with application-transparent support for multiple page sizes,” in *2017 50th Annual IEEE/ACM International Symposium on Microarchitecture (MICRO)*, Oct 2017, pp. 136–150.
- [34] Z. Wang, J. Yang, R. Melhem, B. Childers, Y. Zhang, and M. Guo, “Simultaneous multikernel gpu: Multi-tasking throughput processors via fine-grained sharing,” in *2016 IEEE International Symposium on High Performance Computer Architecture (HPCA)*, March 2016, pp. 358–369.
- [35] C. Gregg, J. Dorn, K. Hazelwood, and K. Skadron, “Fine-grained resource sharing for concurrent gpgpu kernels,” in *Proceedings of the 4th USENIX Conference on Hot Topics in Parallelism*, ser. HotPar’12. Berkeley, CA, USA: USENIX Association, 2012, pp. 10–10. [Online]. Available: <http://dl.acm.org/citation.cfm?id=2342788.2342798>
- [36] R. Ausavarungnirun, V. Miller, J. Landgraf, S. Ghose, J. Gandhi, A. Jog, C. J. Rossbach, and O. Mutlu, “Mask: Redesigning the gpu memory hierarchy to support multi-application concurrency,” *SIGPLAN Not.*, vol. 53, no. 2, pp. 503–518, Mar. 2018. [Online]. Available: <http://doi.acm.org/10.1145/3296957.3173169>